Molecular Cell, Vol. 14, 423–434, May 21, 2004, Copyright ©2004 by Cell Press

GroEL Mediates Protein Folding with a Two Successive Timer Mechanism

Taro Ueno,[1,4] Hideki Taguchi,[2,3,4,5] Hisashi Tadakuma,[1] Masasuke Yoshida,[2,*] and Takashi Funatsu[1,*]
[1]Department of Physics
School of Science and Engineering
Waseda University
3-4-1 Okubo
Tokyo 169-8555
[2]Chemical Resources Laboratory
Tokyo Institute of Technology
4259 Nagatsuta
Yokohama 226-8503
[3]Precursory Research for Embryonic Science and Technology (PRESTO)
JST
Kawaguchi-shi, Saitama 332-0012
Japan

Summary

GroEL encapsulates nonnative substrate proteins in a central cavity capped by GroES, providing a safe folding cage. Conventional models assume that a single timer lasting ~8 s governs the ATP hydrolysis-driven GroEL chaperonin cycle. We examine single molecule imaging of GFP folding within the cavity, binding release dynamics of GroEL-GroES, ensemble measurements of GroEL/substrate FRET, and the initial kinetics of GroEL ATPase activity. We conclude that the cycle consists of two successive timers of ~3 s and ~5 s duration. During the first timer, GroEL is bound to ATP, substrate protein, and GroES. When the first timer ends, the substrate protein is released into the central cavity and folding begins. ATP hydrolysis and phosphate release immediately follow this transition. ADP, GroES, and substrate depart GroEL after the second timer is complete. This mechanism explains how GroES binding to a GroEL-substrate complex encapsulates the substrate rather than allowing it to escape into solution.

Introduction

In prokaryotes and eukaryotes, chaperonins facilitate folding of newly translated, newly translocated, or stress-damaged proteins in an ATP-dependent manner. The best-studied of these chaperonins is the *Escherichia coli* GroEL and its cochaperonin GroES (Bukau and Horwich, 1998; Sigler et al., 1998; Thirumalai and Lorimer, 2001; Hartl and Hayer-Hartl, 2002; Saibil and Ranson, 2002). GroEL comprises 14 identical 57 kDa subunits each containing a site for binding and hydrolysis of ATP (Braig et al., 1994; Boisvert et al., 1996). Seven GroEL subunits are arranged in a heptamer ring forming a central cavity, and two heptamer rings are stacked back to back (Braig et al., 1994). GroES is a dome-shaped, single heptamer ring of 10 kDa subunits (Hunt et al., 1996; Xu et al., 1997).

GroEL binds a wide range of nonnative proteins at the apical cavity rim (Viitanen et al., 1992; Horwich et al., 1993; Fenton et al., 1994; Ewalt et al., 1997; Houry et al., 1999), then subsequently binds ATP and GroES to the same (*cis*) GroEL ring (Xu et al., 1997), producing the *cis* ternary complex consisting of GroEL, nonnative protein, and GroES (Weissman et al., 1995; Mayhew et al., 1996). Since the residues of GroEL involved in GroES binding mostly overlap with those responsible for substrate protein binding (Fenton et al., 1994), it is presumed that, when GroES binds to GroEL, residues within GroES assume responsibility for binding from substrate protein. Then, instead of escaping into the bulk medium, nonnative protein is somehow guided into the cavity of the *cis* ring beneath GroES (the *cis* cavity) where it can initiate folding without risk of aggregation (Fenton et al., 1994; Xu et al., 1997; Chen and Sigler, 1999). As ATPs in the *cis* ring are hydrolyzed to ADP, the opposite side (*trans*) ring of GroEL becomes ready for binding nonnative proteins and ATP, which, in turn, induces the release of GroES, ADP, and substrate protein (whether folded or not) from the *cis* ring (Rye et al., 1997, 1999). Then the *trans* ring subsequently binds GroES, becoming a new *cis* ternary complex for the next chaperonin cycle (Rye et al., 1997, 1999). The functional GroEL cycle proceeds at maximum turnover rate, ~0.12 s^{-1}, when saturating amounts of GroES, ATP, and nonnative proteins are present (Burston et al., 1995; Rye et al., 1999). Under these optimum conditions, binding of these components to GroEL is very rapid, and, according to current model, the whole cycle of GroEL is actually governed by a single rate constant (0.12 s^{-1}) corresponding to the rate of ATP hydrolysis in the *cis* ring (the single timer model) (Weissman et al., 1996; Rye et al., 1997, 1999). Therefore, when the cycle is initiated by addition of ATP to the mixture of GroEL, substrate protein, and GroES, the folding-active *cis* ternary complex should form immediately and all subsequent events, including those of ATP hydrolysis reactions (cleavage of bound ATP, release of ADP and Pi) and decay of the *cis* ternary complex (release of GroES and substrate protein from GroEL), should take place apparently with a single rate constant, ~0.12 s^{-1}. As a result, the substrate protein can utilize almost the whole functional GroEL cycle of ~8 s [lifetime, 1/(0.12 s^{-1})] for productive folding.

However, single molecule imaging of dynamic binding release kinetics of GroES during steady-state functional GroEL cycle has revealed that release of GroES from GroEL occurs through two steps defined by rate constants, ~0.3 s^{-1} and ~0.2 s^{-1} (Taguchi et al., 2001). Typically, GroES binds very rapidly to GroEL, remains for ~3 s (lag period), and departs GroEL over ~5 s (Taguchi et al., 2001). Similar "two timer" kinetics of the

*Correspondence: myoshida@res.titech.ac.jp (M.Y.); funatsu@mol.f.u-tokyo.ac.jp (T.F.)
[4]These authors contributed equally to this work.
[5]Present address: Department of Integrated Biosciences, Graduate School of Frontier Sciences, The University of Tokyo, Kashiwa, Chiba 277-8562, Japan.

release of GroES from GroEL were observed by rapid scanning atomic force microscopy (Viani et al., 2000). These observations are in contrast to the prediction by the single timer model. This is not a trivial contradiction of kinetics because the appearance of another rate constant means the existence of a previously unnoticed intermediate in the functional GroEL cycle that would considerably improve our understanding on the GroEL mechanism. Indeed, a mutant GroEL that did not fit any of the intermediates in the single timer model has been reported (Kawata et al., 1999; Miyazaki et al., 2002).

Despite of a number of reports on GroEL kinetics, there is very little data which might distinguish the single timer model and the two timer model. Here, we report results on the kinetics of the functional GroEL cycle in the presence of ATP, GroES, and nonnative substrate proteins. For this purpose, we have developed a real-time, single molecule observation system for folding of green fluorescent protein (GFP) in the *cis* cavity and found that protein folding started after a lag period of ~3 s. Rearrangements of substrate protein in the *cis* cavity on this time scale were observed for GFP and malate dehydrogenase (MDH) by fluorescence resonance energy transfer (FRET). A second kinetic step necessitated the formation of new intermediates in the functional GroEL cycle, and initial pre-steady-state ATPase kinetics further clarified nucleotide states of these intermediates. This two timer mechanism may provide a possible explanation for the difficult problem of how GroEL can confine a substrate protein within the narrow *cis* cavity.

Results

Single Molecule Imaging Revealed that GFP Folding Was Arrested for the First ~3 s in the *cis* Ternary Complex

To analyze the events in a functional GroEL cycle, we need to monitor the recovery of the activity of the substrate protein in the *cis* cavity as a mark of completion of folding, with a time resolution of s, rather than min. Many studies on the time courses of GroEL(GroES)-mediated protein folding have been published, but few have reported such measurements. The substrate protein for this purpose should exhibit monomer activity that can be measured continuously while it is confined in the *cis* cavity. Since GFP exclusively satisfies these criteria, we developed a real-time, single molecule imaging system to observe folding of GFP in the *cis* cavity (Figure 1A). To immobilize and visualize GroEL, Asp490, which is located at the external surface of GroEL, was replaced by Cys (the mutant was termed EL490) and labeled with biotin-maleimide and IC5-maleimide at the same time. Labeled EL490, as well as unlabeled EL490, behaves like the wild-type GroEL as assessed by every analysis performed, including steady-state ATP hydrolysis and assisted folding of rhodanese and GFP as described previously (Taguchi et al., 2001). In addition, the second mutation D398A was introduced to EL490, termed EL398/490. Like a D398A mutant of GroEL, EL398/490 forms a *cis* ternary complex normally, but it hydrolyzes ATP very slowly, only 2% of wild-type (Rye et al., 1997). In the absence of ATP hydrolysis, EL398/490 keeps GFP in the *cis* cavity up to ~30 min where GFP can complete folding. GFP was denatured in 0.1 M HCl and diluted into a solution of neutral pH containing EL398/490 to form the EL398/490-GFP complex. The complex was infused into a flow cell and immobilized on the glass surface through biotin-streptavidin linker. The glass chamber was then filled with the solution containing GroES and caged ATP. First, the positions of EL398/490 molecules were determined by the fluorescence of IC5 using a total internal reflection fluorescence microscopy (TIRFM) (Figure 1B, "GroEL"). The functional GroEL cycle was triggered by generation of ATP from caged ATP (1 mM) on UV flash. About 40% of caged ATP was converted to ATP. As concentrations of generated ATP and GroES (1 μM) were saturating, their binding to GroEL should not limit the rate but should complete within 0.1 s, as calculated from the binding rate constants and concentrations (Taguchi et al., 2001). Following the photogeneration of ATP, fluorescent spots of the folded GFP appeared over time at the positions of EL398/490 (Figure 1B, "GFP"). Fluorescent spots of GFP that appeared at positions other than preassigned GroEL ones were ascribed to EL398/490 without the IC5 label. Folded GFP in the medium, if any, was not detected due to Brownian motion. All fluorescent spots were of the folded GFP within the *cis* ternary complex since no spots appeared in the absence of GroES.

A histogram of the waiting time for the appearance of GFP fluorescence showed a nonexponential distribution with a maximum at ~8 s (Figure 1C). The same data was replotted as the time course of the accumulated number of fluorescent GFP after UV flash (Figure 1C, inset) to compare with those of the following bulk phase experiments (Figure 2). The data shown in Figure 1C is well described by Equation 1 containing two transitions:

$$\text{denatured GFP*} \xrightarrow{k} \text{denatured GFP} \xrightarrow{k'} \text{native GFP} \quad (1)$$

A simulation of Equation 1 was plotted in Figure 1C with $k = 0.31\ s^{-1}$ and $k' = 0.034\ s^{-1}$ and, therefore, the lifetimes (the reciprocal of the rate constant) of "denatured GFP*" and "denatured GFP" were ~3 and ~33 s, respectively. This means that folding of GFP is arrested during the first ~3 s after GroES binds GroEL.

To avoid argument that these features are specific for the ATPase-deficient mutant, similar experiments were also performed using EL490. EL490 undergoes the normal functional GroEL cycle, and most GFP should be released into the bulk medium before folding is completed. Therefore, to keep maximum GFP in the *cis* cavity during the measuring time, we included apyrase in the reaction mixture to exhaust ATP within ~1 s after the UV flash so that the release of GroES from GroEL was suppressed by the lack of ATP for binding the *trans* ring (Rye et al., 1997, 1999). A histogram of the waiting time for the appearance of GFP fluorescence at the positions of EL490 after photogeneration of ATP showed a nonexponential distribution with a maximum at ~5 s (Figure 1D). The pattern of this histogram differed significantly from that of EL398/490. We measured the time course of the GroES release in the presence of apyrase using Cy3-GroES in a parallel experiment under the same conditions and calibrated the original data, taking into ac-

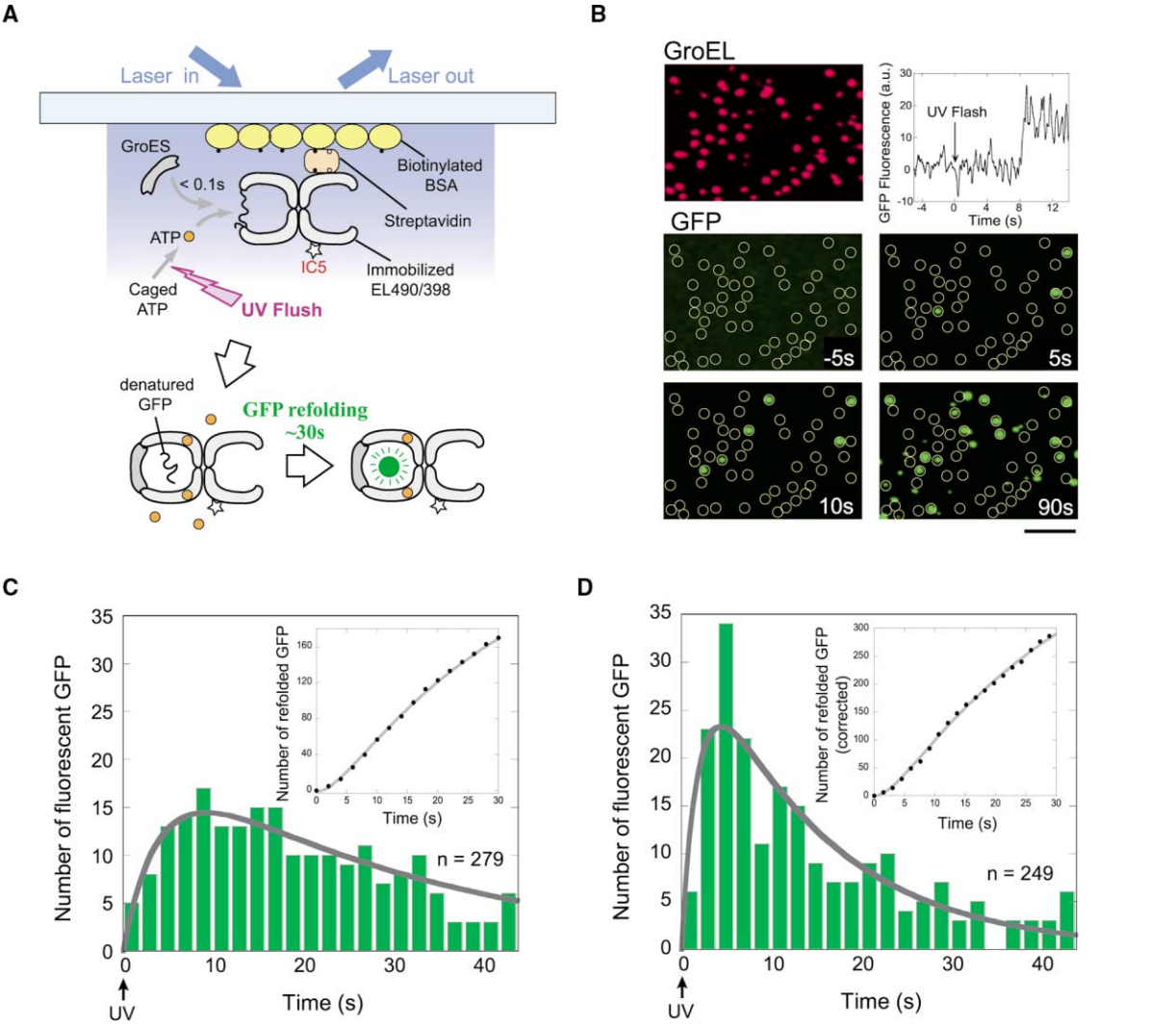

Figure 1. Imaging of Folding of Single Molecule GFP in the *cis* Cavity

(A) Schematic illustration of the experiment. The IC5-GroEL-denatured GFP complex was immobilized on the glass, and ATP was generated from caged ATP by a UV flash in the presence of a saturating amount of GroES. Appearance of GFP at the positions of GroEL was observed with TIRFM.

(B) Fluorescence images of GroEL molecules (GroEL) and GFP molecules (GFP), which folded within the *cis* cavity. ATP was generated at time 0 s. Positions of EL398/490 were indicated by circles colored yellow. Scale bar, 5 μm. (Inset) Time course of the fluorescence intensity of a GFP molecule at the position of GroEL (see Supplemental Movie S1 at http://www.molecule.org/cgi/content/full/14/4/423/DC1).

(C and D) Histograms of the time required for each GFP to gain native structure in (C) EL398/490 or (D) EL490, after the photogeneration of ATP. The solid line is the convolution of two exponentials, $Ck\,k'\,[\exp(-kt) - \exp(-k't)]/(k - k')$, fit to the data by least-squares fitting. This formula is derived from the two-step reaction of Equation 1. (Inset) Time course of the cumulative number of folded GFP molecules. Solid line is the integration of the above formula.

count the premature release of GFP. Including this correction, the histogram fit the two sequential transitions of Equation 1 with $k = 0.34\ s^{-1}$ and $k' = 0.029\ s^{-1}$ (gray line). The result again indicates that folding of denatured GFP in the *cis* ternary complex is arrested for ~3 s before it begins to regain the native conformation in the course of ~30 s. If the lag of ~3 s comes not from substrate release but from the kinetics of GFP refolding after release, the data in Figures 1 and 2 would be the remarkable evidence that the kinetics of protein refolding in the chaperonin cavity is completely different from those in free solution.

Bulk Phase Experiments Also Showed a ~3 s Lag of GFP Folding in the *cis* Ternary Complex

GFP folding was also monitored in bulk phase solution using a fluorometer (Figure 2A). Spontaneous folding, initiated by diluting acid-denatured GFP into a buffer of neutral pH, occurred with a single rate constant $0.032\ s^{-1}$. In this case, no lag was evident (Figure 2B). For GroEL-mediated GFP folding, acid-denatured GFP was diluted to a buffer containing GroEL and GroES to form the GroEL-GFP complex, and the functional GroEL cycle was initiated by addition of ATP. We tested three types of GroEL: EL490, EL398, and a single ring version

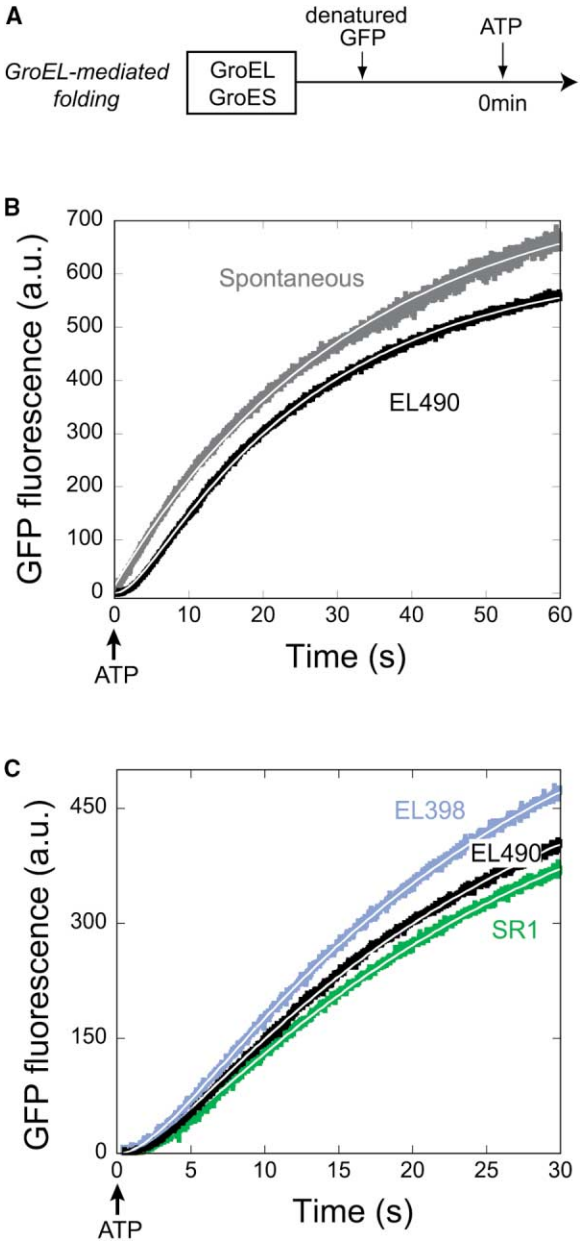

Figure 2. Bulk Phase Measurement of GFP Folding

(A) Diagram of experiments. GFP folding was initiated by adding ATP at 0 s to a buffer A containing GroES and the EL490-denatured GFP complex. Spontaneous folding of GFP was initiated by diluting acid-denatured GFP into buffer A.

(B) Spontaneous GFP folding and GFP folding in the presence of EL490. Spontaneous folding was fit by a single exponential. GFP folding in the presence of EL490 is fit to the data by the convolution of two exponentials.

(C) GFP folding in the presence of EL490, EL398, or SR1.

of GroEL (SR1) (Weissman et al., 1995). In the latter two cases, GFP was not released to the medium but remained in the *cis* cavity due to deficient ATPase (EL398) or lack of the signal from the *trans* ring (SR1). For every GroEL tested, folding of GFP started with an initial lag (Figures 2B and 2C). The time courses were well simulated by Equation 1, and rate constants of GFP folding mediated by EL490, EL398, and SR1 were obtained as $k = 0.35$, 0.35, and 0.30 s^{-1} and $k' = 0.038$, 0.040, and 0.037 s^{-1}, respectively. Simulated lines are shown by solid lines in Figure 2B. Thus, folding kinetics in the bulk phase experiments were very similar to those observed by single molecule imaging. A comment should be added that the results with SR1 appear to exclude the involvement of the *trans* ring in the initial kinetics of GFP folding.

Lags in GFP Folding and GroES Release Varied in the Same Way at Different Temperatures

We previously demonstrated single molecule imaging of binding-release dynamics of GroEL-GroES complex in the functional GroEL cycle (Taguchi et al., 2001). Analysis showed that, without added nonnative protein, release of GroES from GroEL occurred very slowly, but with added nonnative protein, GroES left GroEL in several seconds through two successive steps (Equation 2).

$$[\text{ES-EL}]^* \xrightarrow[k]{} [\text{ES-EL}] \xrightarrow[k']{} [\text{ES}] + [\text{EL}] \qquad (2)$$

Very similar rate constants were obtained for four kinds of nonnative substrate proteins. These were $k = 0.26$–0.34 s^{-1} and $k' = 0.18$–0.24 s^{-1}, that is, GroES remains bound to GroEL for ~3 s and then leaves GroEL in ~5 s, independent of species of nonnative protein. These values were not affected by GroES concentrations in the medium (Taguchi et al., 2001). Since the ~3 s lag coincided with that of GFP folding, we postulated that it probably reflected the same transition of the *cis* ternary complex.

To confirm this, we examined whether the lag in GroES release and GFP folding varied in the same way at different temperatures. Single molecule imaging of GroES binding and release was carried out as described (Taguchi et al., 2001) (Figure 3A). To supply nonnative protein during the observation period, pepsin, a permanently denatured protein at neutral pH (Aoki et al., 1997), was used as a substrate protein. Because GroES release kinetics are largely unaffected by the species of nonnative protein (Taguchi et al., 2001), we compared the kinetics of GroES release in the presence of pepsin to those of GFP folding. Binding and release of individual Cy3-ES molecules to IC5-EL490 were visualized by TIRFM at 18°C, 23°C, and 28°C. Histograms of the duration of bound state (on time) were simulated by Equation 2. The first rate constants (k) were 0.19, 0.33, and 0.44 s^{-1}, and the second rate constants (k') were 0.086, 0.14, and 0.21 s^{-1} at 18°C, 23°C, and 28°C, respectively (Figure 3B). The values increased in parallel with temperature. GFP folding was observed by single molecule imaging with ATPase-deficient EL398 and with EL490 under single turnover conditions by ATP quenching with apyrase. Bulk phase GFP folding also was measured. Plots of rate constants corresponding to the initial lags of GroES-release kinetics and those of GFP folding clearly showed that the values agreed fairly well at all three temperatures (Figure 3C). These results indicate that lag of GroES release and the lag of GFP folding reflects the same transition in the *cis* ternary complex.

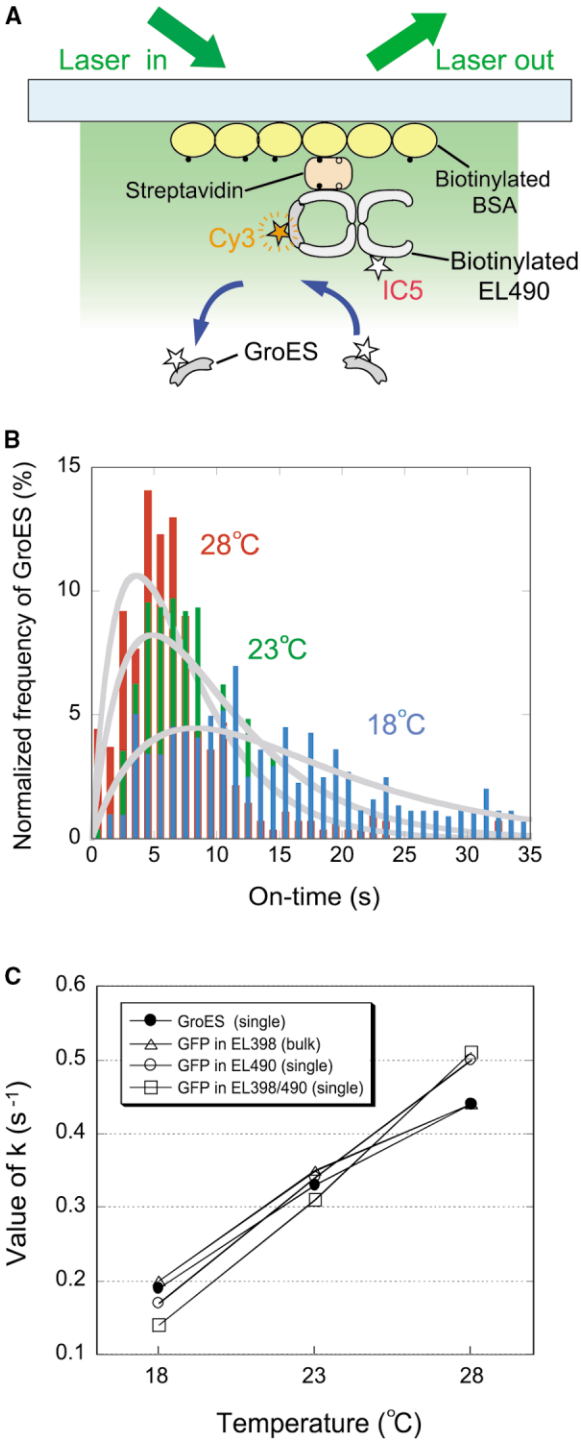

Figure 3. Temperature Dependency of the Lag Period of GFP Folding and that of GroES Release

(A) Schematic illustration of the single molecule imaging of the GroEL-GroES dynamics. Cy3-GroES was seen as a spot only when it bound to EL490 ("on time").

(B) Histograms of duration of GroES on time at different temperatures. The solid lines are the convolution of two exponentials fit to the data by least-squares fitting.

(C) The rate constants that determined the lag period in GroEL-GroES dynamics (*k* in Equation 2) and GFP folding (*k* in Equation 1) at three temperatures.

Bulk Phase Experiments Showed that FRET between Substrate Protein and GroEL Underwent Two Transitions after an Initial Rapid Change

As described above, GFP undergoes a ~3 s folding-arrested state in the initial *cis* ternary complex. To investigate whether this effect is specific for GFP or common to all substrate proteins, similar measurements for other substrate proteins should be performed. However, at present, rapid monitoring of the activity recovery of substrate protein in the *cis* ternary complex has been possible only for GFP, both for bulk phase experiment or single molecule imaging, due to technical difficulties. Instead of activity recovery, we performed ensemble measurement of the changes in fluorescence resonance energy transfer (FRET) between a substrate protein and the apical domain of GroEL (Figure 4A) as the transition of substrate protein from folding-arrested state to folding-competent state should accompany rearrangement of substrate protein in the *cis* ternary complex.

At first, the ensemble of FRET behavior of Cy3-labeled GFP was examined. The Cy3-GFP retained folding ability but recovered GFP fluorescence did not interfere with FRET measurement. A mutant GroEL, in which Glu315 at the apical domain was replaced with Cys (termed EL315) (Rye et al., 1999), was used for the specific labeling of an acceptor dye, IC5. EL315 and IC5-EL315 retained normal ATPase and chaperone activities of GroEL (data not shown). Cy3-GFP was denatured by 0.1 M HCl and diluted into a buffer containing IC5-EL315 to form a complex of Cy3-GFP and IC5-EL315. Then the fluorescence intensity of Cy3-GFP in the presence of EL315 with or without IC5 label was measured by a spectrometer to determine the efficiency of FRET. Upon formation of the complex Cy3-GFP and IC5-EL315, fluorescence intensity of the donor per acceptor decreased to 39% of that in the absence of acceptors, reflecting the close proximity of two dyes.

The GroEL cycle was initiated in the presence and absence of GroES by addition of ATP to the preformed Cy3-GFP-IC5-EL315 complex. In the absence of GroES, fluorescence intensity of the donor increased exponentially at a rate constant 0.13 s^{-1}, reflecting the simple release of Cy3-GFP from IC5-EL315. In the presence of GroES, by contrast, fluorescence intensity of the donor changed in three phases. An initial rapid increase transiently slowed, then increased again. The time course was simulated by assuming three rate constants, 2.1, 0.33, and 0.30 s^{-1} (Figure 4B). The first rate constant may represent a rapid transition that is included in the ~3 s lag. The second may represent the same transition that we observed as a lag in GFP folding. The third may correspond to the release of GFP into bulk solution.

Next, similar experiments were performed using MDH, a stringent substrate protein that folds efficiently only in the presence of GroEL, GroES, and ATP (Peralta et al., 1994; Chen et al., 2001). MDH was labeled with donor dye and Bodipy FL, and the labeled MDH (FL-MDH) retained the ability to fold within GroEL. FL-MDH was denatured in 6.4 M urea and diluted into the buffer containing IC5-EL315 to form a complex. Upon formation of the FL-MDH-IC5-EL315 complex, the fluorescence intensity of the donor per acceptor decreased to 51% of that in the absence of acceptors. The functional GroEL cycle was initiated by addition of ATP to the preformed

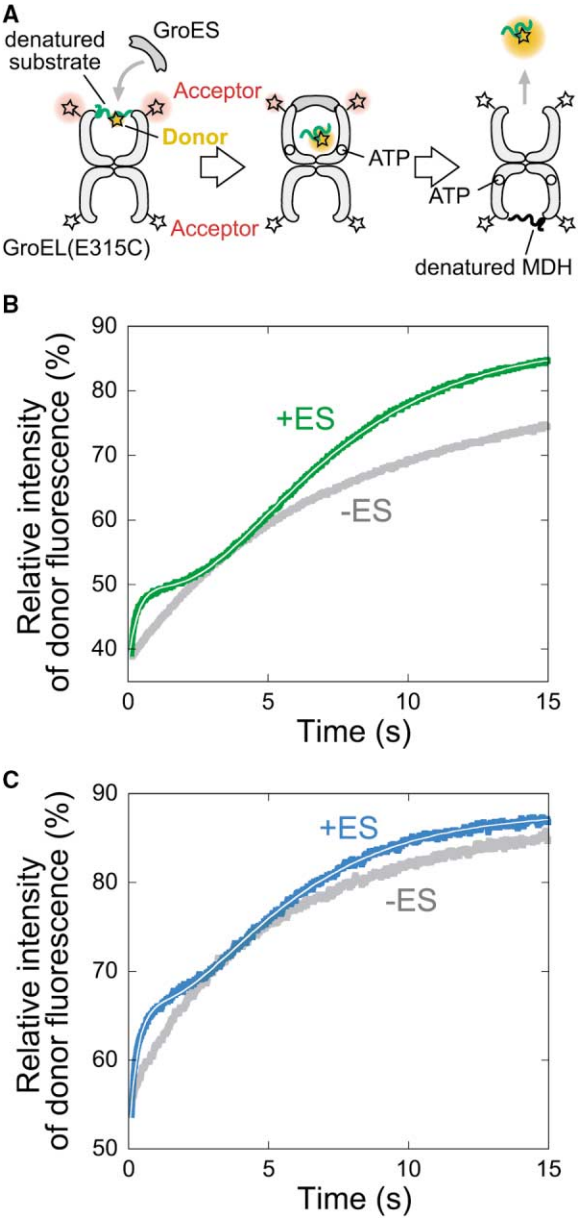

Figure 4. Bulk Phase Measurement of FRET between a Nonnative Protein and the Apical Domain of GroEL

(A) Schematic illustration of the FRET experiment. Denatured substrate protein with donor dye was trapped by EL315 with acceptor dyes. The functional GroEL cycle was initiated by addition of GroES, ATP, and excess nonlabeled denatured MDH to prevent rebinding of labeled denatured protein to EL315.

(B and C) Ensemble of the time course of the relative fluorescence intensity of (B) Cy3-GFP or (C) FL-MDH in the presence or absence of GroES. It was obtained from the ratio of the fluorescence of donor in the presence or absence of acceptor. The data were fit by assuming three-step reactions. Solid lines are the following functions. $D_4 + (D_1 - D_4) \exp(-k_1 t) + (D_2 - D_4) k_1/(k_1 - k_2) [\exp(-k_2 t) - \exp(-k_1 t)] + (D_3 - D_4) k_1 k_2/(k_1 - k_2)/(k_2 - k_3)/(k_1 - k_3) [(k_2 - k_3) \exp(-k_1 t) - (k_1 - k_3) \exp(-k_2 t) + (k_1 - k_2) \exp(-k_3 t)]$. Parameters k_1, k_2, and k_3 are rate constants of a three-step reaction. D_1, D_2, D_3, and D_4 are percentages of donor fluorescence intensity.

FL-MDH-IC5-EL315 complex and GroES. The fluorescence intensity of the donor increased exponentially with a rate constant of 0.19 s^{-1} in the absence of GroES. In the presence of GroES, however, the intensity changed in three phases described by three rate constants, 2.9, 0.46, and 0.31 s^{-1} (Figure 4B). We also carried out experiments using Cy3-labeled MDH and obtained the three rate constants very similar to those with FL-MDH (data not shown). These results are similar to those obtained for the Cy3-GFP and indicate that the substrate protein-GroEL interaction changes in a characteristic manner, including a step that would be corresponding to the ~3 s lag observed in GFP folding kinetics.

Bulk Phase Experiments Showed that ATP Hydrolysis and Pi Release Are Described by the First Rate Constant and ADP Release by the Second Rate Constant

The results shown so far argue that the functional GroEL cycle proceeds with two major rate constants under optimum conditions. Since the whole cycle is driven by ATP hydrolysis, these two rate constants should correlate with the steps in ATPase cycle of GroEL. Although a number of studies on ATPase kinetics of GroEL and GroEL-GroES have been reported, all of these focused on ATPase activity in the absence of nonnative substrate protein (e.g., Todd et al., 1994; Cliff et al., 1999). Consequently, we performed ensemble measurements of the initial pre-steady-state time course of the ATPase cycle of GroEL in the presence of GroES and nonnative proteins. We employed three different assays (Figure 5A) to investigate each stage of the ATPase cycle. Hydrolytic cleavage of a β-γ bond of ATP was measured by total Pi generation with the malachite green method after the reaction was quenched by acid (Geladopoulos et al., 1991). This actually represents the progress of hydrolysis of GroEL-bound ATP. The release of Pi from GroEL was monitored by the Pi binding protein that captured free Pi in the medium and emitted enhanced fluorescence (Brune et al., 1994). Finally, release of ADP from GroEL was monitored by the appearance of free ADP in the medium by the oxidation of NADH with ATP regenerating auxiliary enzymes, pyruvate kinase, and lactate dehydrogenase (Pullman et al., 1960).

The results of total Pi generation are shown in Figure 5B. In the absence of GroES, Pi generation proceeded linearly with a single rate constant of 0.18 s^{-1} (gray line), but, in the presence of GroES, Pi generation started with an initial burst and reached a steady-state turnover (0.12 s^{-1}). The time course is consistent with Equation 3.

$$\begin{array}{c} [\text{ES-EL-ATP}] \xrightarrow[k]{} [\text{ES-EL-ADP-Pi}] \xrightarrow[k']{} \\ [\text{ES}] + [\text{EL}] + [\text{ADP}] + [\text{Pi}] \end{array} \quad (3)$$

The ATPase cycle has two steps with characteristic rate constants. ATP hydrolysis accompanies the first step. The solid line in Figure 5B is a simulated time course of the two rate constants, $k = 0.31$ s^{-1} and $k' = 0.16$ s^{-1}.

Similar to total Pi generation, Pi release from GroEL showed an initial burst in the presence of GroES and denatured MDH (Figure 5C). The time course of Pi release was simulated by Equation 4.

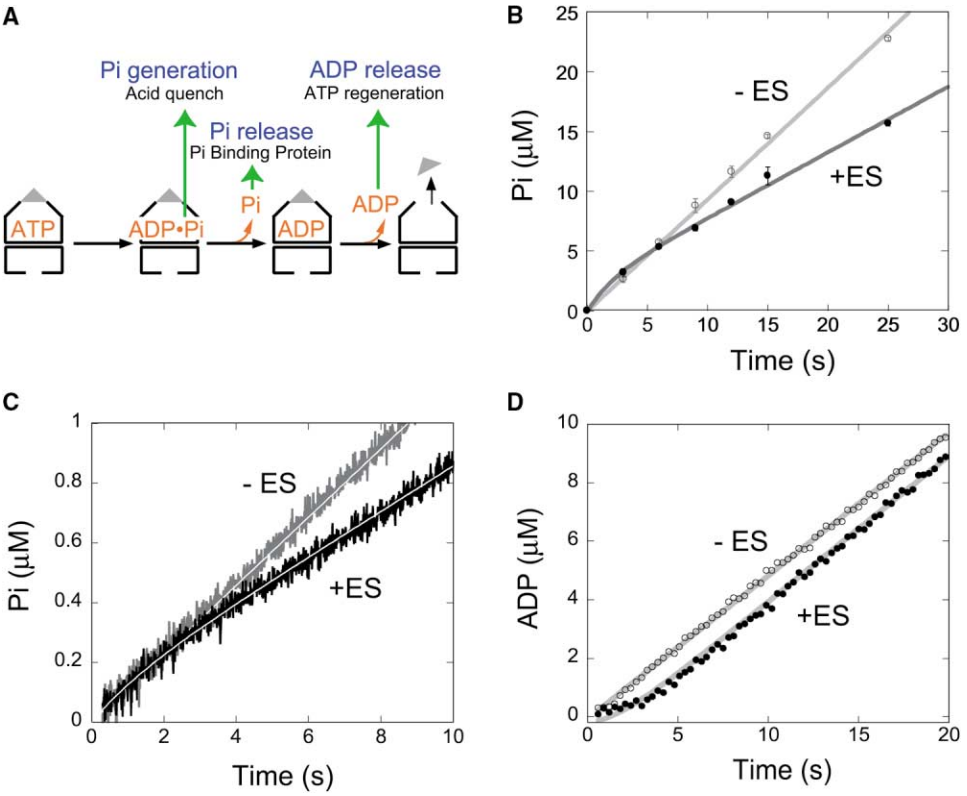

Figure 5. Bulk Phase Measurement of Initial ATPase Kinetics by GroEL in the Presence of Substrate Protein

(A) Schematic illustration of the three assays for ATP hydrolysis by GroEL: Pi generation, Pi release, and ADP release.

(B) Ensemble of the time course of ATP hydrolysis by GroEL in the presence (closed circles) or absence (open circles) of GroES.

(C) Ensemble of the time course of Pi release from GroEL in the presence (black line) or absence (gray line) of GroES.

(D) Ensemble of the time course of ADP release in the presence (black line) or absence (gray line) of GroES. The solid lines fit to the data obtained in the presence of GroES are functions $C_1k\,(k't - k/(k + k')\,\{\exp[-(k + k')t] - 1\})/(k + k')$ in (B) and (C), and $C_2 + k\,k'/(k + k')\,(t + \exp[-(k + k')t]/(k + k')$ in (D). These formulas are derived from the two-step reaction of Equations 3 and 4. The solid lines fit to the data obtained in the absence of GroES are linear functions of $C_3k\,t$.

$$\underset{}{[\text{ES-EL-ATP}]} \xrightarrow[k]{} [\text{ES-EL-ADP}] + [\text{Pi}] \xrightarrow[k']{} [\text{ES}] + [\text{EL}] + [\text{ADP}] + [\text{Pi}] \quad (4)$$

There are two rate constants, $k = 0.33\ s^{-1}$ and $k' = 0.37\ s^{-1}$, and Pi release takes place during the first step defined by k. Using pepsin and reduced α lactalbumin as substrate proteins, we carried out similar experiments and obtained the values $k = 0.36, 0.26\ s^{-1}$ and $k' = 0.46, 0.20\ s^{-1}$, respectively. In the absence of GroES, on the other hand, no burst was observed and the ATPase cycle was defined by a single rate constant of $0.18\ s^{-1}$. The similarity of the k value for total Pi generation and that for Pi release suggests that Pi leaves GroEL immediately after Pi is generated by ATP hydrolysis on GroEL.

The time course of ADP release from GroEL in the presence of GroES and denatured MDH showed the initial lag and then reached the steady-state rate ($0.12\ s^{-1}$) (Figure 5D). The time course was consistent with Equation 4. Two rate constants were calculated as $k = 0.39\ s^{-1}$ and $k' = 0.23\ s^{-1}$, and ADP release occurred at the second transition defined by k'. Without GroES, ADP release proceeded linearly with time. Therefore, one product of ATP hydrolysis, ADP, stays bound for $\sim$4 s after ATP hydrolysis until the next transition in the cycle completes while the other, Pi, leaves GroEL immediately after ATP hydrolysis.

Collectively, the data show that the ATPase cycle of GroEL proceeds with two major rate constants. The first ranges from 0.31 to $0.39\ s^{-1}$ and defines both ATP hydrolysis on GroEL and Pi release from GroEL. The second ranges from 0.16 to $0.37\ s^{-1}$ and governs the ADP release from GroEL. The values of the first rate constant are in close agreement with k values obtained from GFP folding and GroES release. This suggests that the same transition with this rate constant is responsible for the lags of GFP folding, GroES release, and ADP release and for the initial burst of ATP hydrolysis and Pi release. The second rate constants obtained from the ATPase cycle vary but are still in an acceptable range to suggest that they correspond to the rate constants k' obtained from other measurements.

Discussion

Two Timer Mechanism of the Functional GroEL Cycle

The single timer model of the functional GroEL cycle predicts that any events in the cycle after the *cis*-ATP

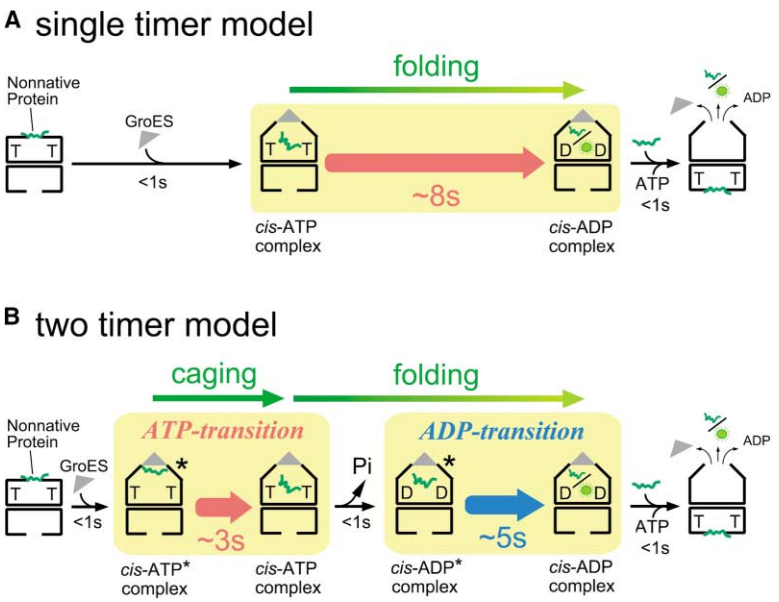

Figure 6. Single Timer Model and Two Timer Model of the Functional GroEL Cycle

(A) Single timer model of GroEL-GroES (Rye et al., 1999). In the presence of saturating amounts of ATP, GroES, and substrate proteins, only a single rate constant governs all events of the functional GroEL cycle, including ATP hydrolysis, release of Pi, ADP, GroES, and substrate protein from GroEL.

(B) Two timer model (this paper). In the presence of saturating amount of ATP, GroES, and substrate proteins, the functional GroEL cycle has two rate-limiting steps, which are represented by arrows colored red and blue. Binding of GroES (gray triangle) to the complex of GroEL-ATP-substrate protein produces the *cis*-ATP* complex in which substrate protein (green) is not fully released into the cavity. The first timer (lifetime, 3 s) is the "ATP transition" from the *cis*-ATP* complex to the *cis*-ATP complex, which results in full release of nonnative protein into the cavity where folding starts. ATP hydrolysis and Pi release of the *cis*-ATP complex occur rapidly to produce the *cis*-ADP* complex. The second timer (lifetime, 5 s) is the ADP transition from the *cis*-ADP* complex to the *cis*-ADP complex. The *cis*-ADP complex can accept ATP to the *trans* GroEL ring that induces rapid decay of the *cis* ternary complex (Rye et al., 1999). Encapsulation (caging) of the substrate protein occurs during ATP transition. Folding occurs in the *cis*-ATP complex and *cis*-ADP* complex.

complex should occur apparently with a single rate constant ~0.12 s^{-1} (lifetime, 8 s) (Figure 6A). This rate constant would correspond to the rate of ATP hydrolysis in the *cis* ring to produce the *cis*-ADP complex, the only rate-limiting step of the whole cycle (Weissman et al., 1996; Rye et al., 1997, 1999). However, all of the results in this report suggest that at least two rate-limiting steps exist in the cycle, and we propose here a model for the functional GroEL cycle, a successive two timer mechanism (Figure 6B). In this model, the GroEL-substrate protein complex binds ATP and GroES to generate the *cis*-ATP* complex in which, different from the *cis*-ATP complex in the single timer model, folding of substrate protein is arrested. The *cis*-ATP* complex is transformed to the *cis*-ATP complex with a rate constant ~0.3 s^{-1} (lifetime, 3 s). As soon as this transition takes place, three events immediately follow: the substrate protein becomes folding competent in the *cis* cavity, ATP is hydrolyzed, and Pi is released. The lifetime of the *cis*-ATP complex is very short, but folding continues in the next *cis*-ADP* complex. The *cis*-ADP* complex is further transformed to the *cis*-ADP complex with a rate constant ~0.2 s^{-1} (lifetime, 5 s). Similar to the *cis*-ADP complex in the single timer model, the *cis*-ADP complex in the two timer model can accept ATP and substrate protein to its *trans* ring, which immediately induces the decay of the *cis* ternary complex, that is, release of GroES, substrate protein, and ADP from the *cis* ring.

The ATP Transition Occurs without ATP Hydrolysis

The two timer mechanism assumes two critical transitions, from the *cis*-ATP* complex to the *cis*-ATP complex (ATP transition) and from the *cis*-ADP* complex to the *cis*-ADP complex (ADP transition) (Figure 6B). To define the ATP transition, it is important to note that an ATPase-deficient mutant EL398 (Figure 2C) or EL398/490 (Figure 1C) can mediate a single round *cis* folding of GFP with the same kinetics, ~3 s lag, as the EL490. This implies that nonnative GFP in the *cis*-ATP* complex reaches a folding-competent state prior to ATP hydrolysis. Therefore, the first rate-limiting step is not ATP hydrolysis. Rather, it is the conformational transition of the *cis*-ATP* complex that accompanies rearrangement of substrate protein from the folding-arrested state to the folding-competent state.

Rearrangement of Substrate Protein during the ATP Transition

The rearrangement of substrate protein in the complex during this transition was detected by FRET between substrate protein and GroEL (Figure 4). After a rapid increase that was not detected by other methods, the donor fluorescence increased with two transitions. The first likely reflects rearrangement of the substrate protein in the ATP transition and the second the decay of the *cis* ternary complex. The FRET time course of GFP and that of MDH are very similar. Likewise, the release kinetics of GroES in the functional GroEL cycle are not affected significantly by the species of substrate protein used: reduced α lactalbumin, an artificial nonstructured protein RP3-42, denatured pepsin, and denatured MDH (Taguchi et al., 2001). It appears that the timer is set only in the presence of substrate protein but ticks independent of the species of the bound substrate proteins. This was assumed in the single timer model, and it is also valid in the two timer model.

Horwich and his colleagues utilized fluorescence anisotropy of pyrene-labeled rhodanese and of intrinsic Trp of Rubisco to probe the rearrangement of substrate protein in the functional GroEL cycle initiated by addition of ATP and GroES to the GroEL-substrate protein complex (Weissman et al., 1996; Rye et al., 1997). For both substrates, two-phase transitions were observed, the first being a sharp drop in anisotropy (half time 1 s =

lifetime 1.4 s) reflecting the change of substrate protein from the restricted state to the flexible state (Weissman et al., 1996; Rye et al., 1997). The researchers assigned the flexible state to the folding-competent state in the *cis*-ATP complex but did not integrate the restricted state in their single timer model. However, we think that the most reasonable candidate for the restricted state might be the folding-arrested state in the *cis*-ATP* complex. The difference of lifetimes, ~1.5 s in their experiment and ~3 s in our model, is significant but acceptable when taking into account differing experimental conditions. Hydrogen exchange of substrate protein during functional GroEL cycle suggested a possible mechanical unfolding step before complete release of substrate protein into the *cis* cavity (Shtilerman et al., 1999). There is a possibility that this step might correspond to the *cis*-ATP* complex, but the short lifetime of this step (<1 s) makes this possibility rather unlikely. In addition, since another report using the same technique did not detect such an unfolding step (Chen et al., 2001), it is not clear that mechanical unfolding is a general step for various substrate proteins.

The Two Timer Mechanism Explains the Burst and Lag in the Initial Kinetics

Initial kinetics of ATP hydrolysis, GFP folding, and release kinetics of GroES in the cycle showed either lag or burst. We showed that upon initiation of the functional GroEL cycle by ATP addition, ATP hydrolysis in the *cis* ring, and release of Pi occurred as an initial burst with rate constant ~0.3 s^{-1} (Figures 5B and 5C). One might think from Figure 6B that there should be a lag rather than a burst for these events, because they occur after an event that has a lifetime of ~3 s. However, in general, if a rapid event follows a first slow event, these two events should be observed as if they occur simultaneously with the same rate constant, and a lag should not be observed in the rapid event. That happened in the case of ATP hydrolysis and Pi release, which occurred apparently at the same rate as that for ATP transition. Because the steady-state rate of ATP hydrolysis and Pi release (0.12 s^{-1}) is much slower than the initial rate (0.3 s^{-1}) due to the presence of the second rate-limiting step (0.2 s^{-1}), an initial burst should appear in the pre-steady-state kinetics. On the other hand, if a second slow event follows the first slow event, the second appears to occur after the lag period that corresponds to the time needed for the completion of the first slow event. This was the case for GFP folding, which showed a ~3 s lag. Following similar reasoning, decay of the *cis*-ADP complex (release of ADP, GroES, and substrate protein from GroEL) should be observed as if it occurs simultaneously with the ADP transition. Therefore, initial time courses of ADP release from GroEL showed a ~3 s lag when the cycle was initiated by addition of ATP.

The *cis*-ATP* Complex Ensures Efficient Caging of Substrate Protein

The essence of chaperonin function is encapsulation of nonnative protein into a narrow cage to facilitate folding in a protected environment (Weissman et al., 1995; Mayhew et al., 1996; Xu et al., 1997; Sakikawa et al., 1999). However, the mechanism of this efficient caging is only poorly understood. According to the single timer model, upon formation of the *cis*-ATP complex, GroES deprives the previously bound substrate protein of common binding sites on GroEL, and the substrate protein is released into the *cis* cavity. In a microscopic view, GroES can bind to GroEL only when nonnative substrate protein is released from GroEL to make the common binding sites available. It is unclear, however, how the release of substrate protein always results in encapsulation into the *cis* cavity rather than diffusing away to the bulk solution. The two timer model can offer rational explanation for the caging of the substrate protein. In the *cis*-ATP* complex, GroES is already bound but nonnative substrate protein remains in the folding-arrested state. This means that the polypeptide chain of the substrate protein should be interacting with the wall of the *cis* cavity. The ATP transition brings about a conformational change and the next intermediate, the *cis*-ATP complex, disfavors the interaction with substrate protein (Chaudhry et al., 2003). The substrate protein is thus set free to the *cis* cavity to start folding. Therefore the *cis*-ATP* complex plays a critical role in caging the substrate protein into the *cis* cavity.

The structural features of the *cis*-ATP* complex are as yet unknown. Intriguingly, the GroEL mutant C138W forms a folding-arrested *cis* ternary complex at 25°C, which can resume the cycle at 37°C (Kawata et al., 1999; Miyazaki et al., 2002). The arrested *cis* ternary complex of this mutant displays features of the *cis*-ATP* complex. It is noteworthy that substrate protein is located in a protease-inaccessible area in this complex. Amino acid residue C138 resides in the intermediate domain of GroEL and introduction of a bulky tryptophan at this position may restrict the hinge motion. One of candidates for the *cis*-ATP* complex could be such a complex in which a hinge of each GroEL subunit is partially "open."

Substrate Protein Is Free to Fold in the *cis*-ADP* Complex

It is well established that the substrate protein in the *cis*-ADP complex is released to the medium rapidly when ATP and nonnative substrate protein are present in the medium (Rye et al., 1999; Taguchi et al., 2001). Therefore, if the next intermediate after the *cis*-ATP complex is the *cis*-ADP complex, nonnative protein has little time to fold in the *cis* cavity. For this reason, a *cis*-ADP* complex, in which nonnative protein can fold, should be present before the *cis*-ADP complex. Our results show that the lifetime of the *cis*-ADP* complex, that is, the mean time given to nonnative protein to fold, is ~5 s. Because these two ADP complexes differ as to whether the *trans* ring can accept ATP or not, the ADP transition may bring about the conformational change mainly in the *trans* ring region. Cryo-electron micrography shows that the largest structural difference between the ATP-containing and ADP-containing GroEL-GroES complex is in the *trans* ring (Rye et al., 1999). This is reminiscent of the difference between *cis*-ADP* and *cis*-ADP complexes.

Both the ATP transition and the ADP transition do not accompany the change of chemical components of the complex. It seems that they are purely conformational

relaxation and that GroEL is at first raised to the "activated state" when it forms the *cis*-ATP* complex, and subsequent relaxation processes are coupled to exertion of the work. If this really is the case, the timers of GroEL are intrinsic ones built within the conformational dynamics.

Experimental Procedures

Proteins and Reagents

Bovine serum albumin, pepsin, glucose oxidase and catalase, "bacterial" purine nucleoside phosphorylase, phosphoenolpyruvate, and 7-methylguanosine were obtained from Sigma. Streptavidin and [2-(1-maleimidyl)ethyl]-7-(diethylamino)-coumarin-3-carboxamide (MDCC) were from Molecular Probes. Porcine heart malate dehydrogenase, rabbit muscle pyruvate kinase, and hog muscle lactate dehydrogenase were from Roche. The GroEL mutants (EL490, EL398, EL398/490, EL315) were produced by site-directed mutagenesis using the Kunkel method. GroEL mutants, GroES and GFP (S65T), were expressed in *Escherichia coli* and purified as described (Makino et al., 1997; Sakikawa et al., 1999; Motojima et al., 2000). GFP (S65T) was used throughout this work. Protein concentrations were determined by absorption spectroscopy using the following extinction coefficients at 280 nm: GroEL mutants 14-mer, 130480 $M^{-1}cm^{-1}$; GroES 7-mer, 8960 $M^{-1}cm^{-1}$; GFP (S65T) monomer, 18850 $M^{-1}cm^{-1}$. Protein concentration was expressed as oligomer (GroEL, 14-mer; SR1, 7-mer; GroES, 7-mer) throughout the study.

Microscopy

Total internal reflection fluorescence microscopy (TIRFM) was used for visualizing individual fluorescent molecules immobilized on the surface of a quartz slide. Single protein molecules labeled with Cy3 or IC5 were illuminated with a green solid-state laser (2.8 mW, 532 nm, μ-green model 4601, Uniphase, USA) or a He-Ne laser (1.0 mW, 632.8 nm, NEC, Japan), respectively. GFP molecules were illuminated with a blue solid-state laser (1.8 mW, 473 nm, HK-5511, Shimadzu Corporation, Japan) to visualize individual molecules. Images were taken by a SIT camera (C2400-08, Hamamatsu Photonics, Japan) coupled to an image intensifier (VS4-1845, Video Scope International, USA) and recorded on videotapes for subsequent analysis.

Imaging of GFP Folding

Folding of individual GFP molecules in GroEL was visualized by TIRFM. Both EL490 and EL398/490 were labeled with IC5-maleimide and biotin-$PEAC_5$-maleimide (Dojindo Laboratories, Japan) in buffer A (25 mM HEPES-KOH [pH 7.4], 100 mM KCl, 5 mM $MgCl_2$) as descrived previously (Taguchi et al., 2001). GFP (54 μM) was denatured for 2 min at 23°C in 0.1 M HCl and diluted to 2 μM with buffer A containing 400 nM EL490. After 5 min, EL490-denatured GFP complexes were infused into a flow cell and attached to the glass surface via streptavidin as described (Taguchi et al., 2001). Then the cell was filled with buffer A containing 1 μM GroES, 1 mM caged ATP, 25 units/ml apyrase, and an oxygen scavenger system (25 mM glucose, 2.5 μM glucose oxidase, 10 nM catalase, 10 mM dithiothreitol). The specimen was illuminated with a He-Ne laser to mark the position of EL490 and illuminated with a blue solid-state laser to visualize fluorescence of GFP. ATP was released by epifluorescence illumination of UV light for 250 ms with a 100 W mercury light source (U-MWU & IX-FLA, Olympus). Approximately 40% of caged ATP was split under the experimental condition, and ATP was hydrolyzed by apyrase in ~1 s. Appearance of the fluorescence of GFP at the position of EL490 after the photolysis of caged ATP was visualized by TIRFM. About 30% of the EL490 particles thus immobilized were active in folding of GFP.

Bulk Phase GFP Folding

In 1.2 ml of buffer A containing 5 mM dithiothreitol, 150 nM GroEL (EL490, EL398, or SR1), and 1.5 μM GroES at 23°C, 3 μl of acid-denatured GFP was diluted to a final concentration of 100 nM. After 15 min, 3 μl of ATP solution was added to a final concentration of 0.45 mM to start GroEL-GroES-assisted GFP folding. Fluorescence intensity of GFP was monitored continuously with a fluorometer (Ex 485 nm/Em 512 nm, F-4500, HITACHI). Dead time for the measurement was about 0.4 s.

Single Molecule Imaging of GroES-GroEL Dynamics

Single molecule imaging of GroEL-GroES dynamics was carried out using TIRFM as described (Taguchi et al., 2001). Experiments were performed at 18°C, 23°C, and 28°C.

Bulk Phase Measurements of FRET between GroEL and Substrate Protein

EL315 was labeled with IC5-maleimide. The molar ratio of IC5-label to the single ring of GroEL was 1.4. GFP was labeled with Cy3-NHS (Amersham-Pharmacia) at a molar ratio of 0.36. MDH was labeled with BodipyFL-SE (Molecular Probes) at a molar ratio of 0.25 per monomer. Cy3-GFP (8.3 μM) was denatured in 0.1 M HCl for 3 min and diluted to a final concentration of 50 nM with buffer A containing 100 nM IC5-EL315 and 5 mM DTT to make the complex of Cy3-GFP and IC5-EL315. After 5 min at 23°C, 3 μM GroES was added. The solution was loaded into a stopped-flow syringe, and buffer A containing 2 mM ATP, 5 mM DTT, and 1 μM denatured MDH was loaded into another syringe. Equal amounts of these solutions were mixed rapidly in a stopped-flow apparatus (RX 2000, Applied Photo Physics, UK) installed in a fluorometer (FP-6500, JASCO, Japan). The dead time for the measurement was about 0.07 s. To detect the fluorescence of Cy3 as a donor, the solution was excited at wavelength of 540 nm and the fluorescence from 565 to 575 nm was collected. A similar experiment was performed using EL315 without IC5 labeling. A time course of the relative intensity of Cy3 fluorescence was obtained from the ratio of Cy3-GFP fluorescence in the presence or absence of IC5-EL315 divided by the labeling ratio of IC5 per single ring of EL315. Förster distances between a Cy3-IC5 pair were expected to be ~4.9 nm (Wu and Brand, 1994). FRET between FL-MDH and IC-EL315 was measured as follows. FL-MDH (2 μM) was denatured in 6.4 M urea for more than 30 min at 23°C. Then it was diluted to the final concentration of 50 nM with buffer A containing 100 nM EL315, 5 mM DTT, and 3 μM GroES. Rapid mixing was performed as described for Cy3-GFP. The sample was excited at wavelength of 475 nm, and fluorescence from 507.5 to 512.5 nm was collected. Förster distances between a Bodipy FL-IC5 pair were expected to be ~4.7 nm.

Bulk Phase Measurements of Pre-Steady-State Kinetics of ATP Hydrolysis

The ATP hydrolysis reaction in the functional GroEL cycle was measured by three different assays at 23°C. Concentrations of the reaction components were varied to adjust the level suitable for each assay method.

Pi Generation

Generation of Pi from GroEL was measured using the malachite green assay (Geladopoulos et al., 1991). MDH (86 μM) denatured in 6 M urea was diluted to 3 μM into buffer A containing 1.5 μM GroEL and 5 mM DTT in the presence or absence of 4.5 μM GroES. After 5 min, 35 μl of the solution was injected into the same volume of buffer A containing 0.4 mM ATP that was vigorously stirred. The reactions were terminated by the addition of perchloric acid at the indicated times. The solution was centrifuged to remove protein precipitates. The supernatant was treated with a malachite green reagent, and the absorbance at 630 nm was measured.

Pi Release

Release of Pi from GroEL was measured using Pi binding protein (PBP) (Brune et al., 1994, 1998; Cliff et al., 1999). PBP labeled with MDCC, a coumarin derivative, was prepared as previously described (Brune et al., 1994, 1998). Binding of Pi to MDCC-labeled PBP (MDCC-PBP) increased the fluorescence emission at 466 nm when the complex was excited at 430 nm. By virtue of rapid binding of Pi to MDCC-PBP ($k_{on} = 1.36 \times 10^8\ M^{-1}\ s^{-1}$) and high affinity of PBP for Pi ($K_d = 0.1$ μM) (Brune et al., 1994, 1998), the increase in the Pi concentration in the solutions could be monitored as the increase of fluorescence emission in real time. To 1.2 ml of buffer A containing 0.07 μM GroEL, 10 μM MDCC-PBP in the presence or absence of 0.57 μM GroES, 12 μl of 60 μM MDH denatured in 6 M urea were added. After a 5 min incubation at 23°C, the solution was vigorously stirred and the reaction was initiated by injection of 1.5 μl ATP

solution, which contained 80 mM ATP, 800 μM 7-methylguanosine, and 0.1 unit/ml purine nucleoside phosphorylase. The latter two components were used to eliminate contaminating Pi. Changes in the fluorescence at 466 nm were monitored continuously with a fluorometer (F-4500, Hitachi).

ADP Release

Release of ADP from GroEL was measured spectrophotometrically with an ATP-regenerating system (Pullman et al., 1960; Kato et al., 1995). The assay mixture consisted of buffer A containing 0.2 mM NADH, 5 mM phosphoenolpyruvate, 100 μg/ml pyruvate kinase, 100 μg/ml lactate dehydrogenase, 2.5 mM DTT, and 1 mM ATP in the presence or absence of 1.4 μM GroES. MDH (47 μM) denatured in 6 M urea was diluted into the assay mixture to a final concentration of 1.0 μM. After 1 min, the reaction was initiated by injection of GroEL into the vigorously stirred solution. The decreases in the absorbance at 340 nm, due to oxidation of NADH, were monitored continuously with a spectrophotometer (V-550, Jasco, Japan).

Acknowledgments

We thank A. Horwich for critical discussion; M. Webb and T. Masaike for the use of the Pi binding protein assay; J. Suzuki and A. Koike for technical assistance; and R. Shiurba for comments on the manuscripts. This work was supported in part by Grants-in-Aid for Scientific Research on Priority Areas (to H.T. and M.Y.), Specially Promoted Research, COE research, the 21th Century COE program (to T.F.), and Scientific Research B (to H.T. and T.F.), from the Ministry of Education, Culture, Sports, Science, and Technology of Japan.

Received: October 2, 2003
Revised: March 29, 2004
Accepted: March 30, 2004
Published: May 20, 2004

References

Aoki, K., Taguchi, H., Shindo, Y., Yoshida, M., Ogasahara, K., Yutani, K., and Tanaka, N. (1997). Calorimetric observation of a GroEL-protein binding reaction with little contribution of hydrophobic interaction. J. Biol. Chem. *272*, 32158–32162.

Boisvert, D.C., Wang, J., Otwinowski, Z., Horwich, A.L., and Sigler, P.B. (1996). The 2.4 Å crystal structure of the bacterial chaperonin GroEL complexed with ATPgS. Nat. Struct. Biol. *3*, 170–177.

Braig, K., Otwinowski, Z., Hegde, R., Boisvert, D.C., Joachimiak, A., Horwich, A.L., and Sigler, P.B. (1994). The crystal structure of the bacterial chaperonin GroEL at 2.8 Å. Nature *371*, 578–586.

Brune, M., Hunter, J.L., Corrie, J.E., and Webb, M.R. (1994). Direct, real-time measurement of rapid inorganic phosphate release using a novel fluorescent probe and its application to actomyosin subfragment 1 ATPase. Biochemistry *33*, 8262–8271.

Brune, M., Hunter, J.L., Howell, S.A., Martin, S.R., Hazlett, T.L., Corrie, J.E., and Webb, M.R. (1998). Mechanism of inorganic phosphate interaction with phosphate binding protein from Escherichia coli. Biochemistry *37*, 10370–10380.

Bukau, B., and Horwich, A.L. (1998). The Hsp70 and Hsp60 chaperone machines. Cell *92*, 351–366.

Burston, S.G., Ranson, N.A., and Clarke, A.R. (1995). The origins and consequences of asymmetry in the chaperonin reaction cycle. J. Mol. Biol. *249*, 138–152.

Chaudhry, C., Farr, G.W., Todd, M.J., Rye, H.S., Brunger, A.T., Adams, P.D., Horwich, A.L., and Sigler, P.B. (2003). Role of the gamma-phosphate of ATP in triggering protein folding by GroEL-GroES: function, structure and energetics. EMBO J. *22*, 4877–4887.

Chen, L., and Sigler, P.B. (1999). The crystal structure of a GroEL/peptide complex: plasticity as a basis for substrate diversity. Cell *99*, 757–768.

Chen, J., Walter, S., Horwich, A.L., and Smith, D.L. (2001). Folding of malate dehydrogenase inside the GroEL-GroES cavity. Nat. Struct. Biol. *8*, 721–728.

Cliff, M.J., Kad, N.M., Hay, N., Lund, P.A., Webb, M.R., Burston, S.G., and Clarke, A.R. (1999). A kinetic analysis of the nucleotide-induced allosteric transitions of GroEL. J. Mol. Biol. *293*, 667–684.

Ewalt, K.L., Hendrick, J.P., Houry, W.A., and Hartl, F.U. (1997). In vivo observation of polypeptide flux through the bacterial chaperonin system. Cell *90*, 491–500.

Fenton, W.A., Kashi, Y., Furtak, K., and Horwich, A.L. (1994). Residues in chaperonin GroEL required for polypeptide binding and release. Nature *371*, 614–619.

Geladopoulos, T.P., Sotiroudis, T.G., and Evangelopoulos, A.E. (1991). A malachite green colorimetric assay for protein phosphatase activity. Anal. Biochem. *192*, 112–116.

Hartl, F.U., and Hayer-Hartl, M. (2002). Molecular chaperones in the cytosol: from nascent chain to folded protein. Science *295*, 1852–1858.

Horwich, A.L., Low, K.B., Fenton, W.A., Hirshfield, I.N., and Furtak, K. (1993). Folding in vivo of bacterial cytoplasmic proteins: role of GroEL. Cell *74*, 909–917.

Houry, W.A., Frishman, D., Eckerskorn, C., Lottspeich, F., and Hartl, F.U. (1999). Identification of in vivo substrates of the chaperonin GroEL. Nature *402*, 147–154.

Hunt, J.F., Weaver, A.J., Landry, S.J., Gierasch, L., and Deisenhofer, J. (1996). The crystal structure of the GroES co-chaperonin at 2.8 Å resolution. Nature *379*, 37–45.

Kato, Y., Sasayama, T., Muneyuki, E., and Yoshida, M. (1995). Analysis of time-dependent change of Escherichia coli F1-ATPase activity and its relationship with apparent negative cooperativity. Biochim. Biophys. Acta *1231*, 275–281.

Kawata, Y., Kawagoe, M., Hongo, K., Miyazaki, T., Higurashi, T., Mizobata, T., and Nagai, J. (1999). Functional communications between the apical and equatorial domains of GroEL through the intermediate domain. Biochemistry *38*, 15731–15740.

Makino, Y., Amada, K., Taguchi, H., and Yoshida, M. (1997). Chaperonin-mediated folding of green fluorescent protein. J. Biol. Chem. *272*, 12468–12474.

Mayhew, M., da Silva, A.C.R., Martin, J., Erdjument-Bromage, H., Tempst, P., and Hartl, F.U. (1996). Protein folding in the central cavity of the GroEL-GroES chaperonin complex. Nature *379*, 420–426.

Miyazaki, T., Yoshimi, T., Furutsu, Y., Hongo, K., Mizobata, T., Kanemori, M., and Kawata, Y. (2002). GroEL-substrate-GroES ternary complexes are an important transient intermediate of the chaperonin cycle. J. Biol. Chem. *277*, 50621–50628.

Motojima, F., Makio, T., Aoki, K., Makino, Y., Kuwajima, K., and Yoshida, M. (2000). Hydrophilic residues at the apical domain of GroEL contribute to GroES binding but attenuate polypeptide binding. Biochem. Biophys. Res. Commun. *267*, 842–849.

Peralta, D., Hartman, D.J., Hoogenraad, N.J., and Hoj, P.B. (1994). Generation of a stable folding intermediate which can be rescued by the chaperonins GroEL and GroES. FEBS Lett. *339*, 45–49.

Pullman, M.E., Penefsky, H.S., Datta, A., and Racker, E. (1960). Partial resolution of the enzymes catalyzing oxidative phosphorylation. J. Biol. Chem. *235*, 3322–3329.

Rye, H.S., Burston, S.G., Fenton, W.A., Beechem, J.M., Xu, Z., Sigler, P.B., and Horwich, A.L. (1997). Distinct actions of *cis* and *trans* ATP within the double ring of the chaperonin GroEL. Nature *388*, 792–798.

Rye, H.S., Roseman, A.M., Chen, S., Furtak, K., Fenton, W.A., Saibil, H.R., and Horwich, A.L. (1999). GroEL-GroES cycling: ATP and nonnative polypeptide direct alternation of folding-active rings. Cell *97*, 325–338.

Saibil, H.R., and Ranson, N.A. (2002). The chaperonin folding machine. Trends Biochem. Sci. *27*, 627–632.

Sakikawa, C., Taguchi, H., Makino, Y., and Yoshida, M. (1999). On the maximum size of proteins to stay and fold in the cavity of GroEL underneath GroES. J. Biol. Chem. *274*, 21251–21256.

Shtilerman, M., Lorimer, G.H., and Englander, S.W. (1999). Chaperonin function: folding by forced unfolding. Science *284*, 822–825.

Sigler, P.B., Xu, Z., Rye, H.S., Burston, S.G., Fenton, W.A., and Horwich, A.L. (1998). Structure and function in GroEL-mediated protein folding. Annu. Rev. Biochem. *67*, 581–608.

Taguchi, H., Ueno, T., Tadakuma, H., Yoshida, M., and Funatsu, T. (2001). Single-molecule observation of protein-protein interactions in the chaperonin system. Nat. Biotechnol. *19*, 861–865.

Thirumalai, D., and Lorimer, G.H. (2001). Chaperonin-mediated protein folding. Annu. Rev. Biophys. Biomol. Struct. *30*, 245–269.

Todd, M.J., Viitanen, P.V., and Lorimer, G.H. (1994). Dynamics of the chaperonin ATPase cycle: implications for facilitated protein folding. Science *265*, 659–666.

Viani, M.B., Pietrasanta, L.I., Thompson, J.B., Chand, A., Gebeshuber, I.C., Kindt, J.H., Richter, M., Hansma, H.G., and Hansma, P.K. (2000). Probing protein-protein interactions in real time. Nat. Struct. Biol. *7*, 644–647.

Viitanen, P.V., Gatenby, A.A., and Lorimer, G.H. (1992). Purified GroEL interacts with the non-native states of a multitude of E. coli proteins. Protein Sci. *1*, 361–369.

Weissman, J.S., Hohl, C.M., Kovalenko, O., Kashi, Y., Chen, S., Braig, K., Saibil, H.R., Fenton, W.A., and Horwich, A.L. (1995). Mechanism of GroEL action: productive release of polypeptide from a sequestered position under GroES. Cell *83*, 577–587.

Weissman, J.S., Rye, H.S., Fenton, W.A., Beechem, J.M., and Horwich, A.L. (1996). Characterization of the active intermediate of a GroEL-GroES-mediated protein folding reaction. Cell *84*, 481–490.

Wu, P.G., and Brand, L. (1994). Resonance energy transfer: methods and applications. Anal. Biochem. *218*, 1–13.

Xu, Z., Horwich, A.L., and Sigler, P.B. (1997). The crystal structure of the asymmetric GroEL-GroES-(ADP)7 chaperonin complex. Nature *388*, 741–750.